RESEARCH ARTICLE | MARCH 28 2017

Influence of dislocation density on internal quantum efficiency of GaN-based semiconductors

Jiadong Yu; Zhibiao Hao ; Linsen Li; Lai Wang ; Yi Luo; Jian Wang; Changzheng Sun; Yanjun Han; Bing Xiong; Hongtao Li

AIP Advances 7, 035321 (2017)
https://doi.org/10.1063/1.4979504

Influence of dislocation density on internal quantum efficiency of GaN-based semiconductors

Jiadong Yu, Zhibiao Hao,[a] Linsen Li, Lai Wang, Yi Luo,[b] Jian Wang, Changzheng Sun, Yanjun Han, Bing Xiong, and Hongtao Li
Tsinghua National Laboratory for Information Science and Technology, Department of Electronic Engineering, Tsinghua University, Beijing 100084, China

(Received 25 October 2016; accepted 17 March 2017; published online 28 March 2017)

By considering the effects of stress fields coming from lattice distortion as well as charge fields coming from line charges at edge dislocation cores on radiative recombination of exciton, a model of carriers' radiative and non-radiative recombination has been established in GaN-based semiconductors with certain dislocation density. Using vector average of the stress fields and the charge fields, the relationship between dislocation density and the internal quantum efficiency (IQE) is deduced. Combined with related experimental results, this relationship is fitted well to the trend of IQEs of bulk GaN changing with screw and edge dislocation density, meanwhile its simplified form is fitted well to the IQEs of AlGaN multiple quantum well LEDs with varied threading dislocation densities but the same light emission wavelength. It is believed that this model, suitable for different epitaxy platforms such as MOCVD and MBE, can be used to predict to what extent the luminous efficiency of GaN-based semiconductors can still maintain when the dislocation density increases, so as to provide a reasonable rule of thumb for optimizing the epitaxial growth of GaN-based devices. [http://dx.doi.org/10.1063/1.4979504]

I. INTRODUCTION

As wide bandgap semiconductor materials, GaN-based semiconductors have been widely used for optoelectronic devices (such as LED, laser diode, solar cell, photodetector)[1–4] and electronic devices (such as HEMT, HBT, MISFET, SAW).[5–8] Until now, metal-organic chemical vapor deposition (MOCVD) is the most commonly used method for epitaxial growth of GaN-based semiconductors.[9] When using sapphire (0001), 6H-SiC or Si (111) as the heterogeneous substrate,[10–12] GaN-based semiconductors grown by MOCVD still have high dislocation density of 10^8-10^9 cm^{-2}. In fact, however, the internal quantum efficiency (IQE) of InGaN MQW can reach 80%-90% under small carrier injection, and the IQE changes a little when the dislocation density changes within a certain range.[13–16]

Normally, only threading dislocations act as non-radiative centers and affect the IQE of active layers, while misfit dislocations merged in buffer layers do not affect the IQE. There have been some research on the relationship between dislocation density and IQE, such as the influence of dislocation density on the non-radiative recombination[17,18] and minority carrier diffusion in the dopant material.[14,19] Although these research revealed various physical mechanisms of the impacts of dislocation density on IQE of GaN-based materials, the influence of stress fields as well as charge fields of dislocations on exciton radiative recombination is still need further study. Lattice distortion occurs near dislocation due to the destroyed symmetry of perfect lattice, leading to tensile

[a]Electronic address: zbhao@mail.tsinghua.edu.cn
[b]Electronic address: luoy@mail.tsinghua.edu.cn

strain parallel to the substrate surface and compressive strain along the growth direction.[20] Thus the stress fields will be induced on account of material piezoelectric characteristics. Meanwhile, charge fields will come from the line charge at edge dislocation cores due to dangling bonds.[21] Both stress fields and charge fields have crucial influence on the radiative recombination of exciton which is an important issue that cannot be ignored because it is relatively strong at room temperature in GaN-based semiconductors. Besides, previous reports did not give a specific quantitative relationship between IQE and dislocation density, thus based on very limited experimental data, it is hard to predict the level of IQE when the dislocation density changes. Therefore, it is necessary to understand the influence of dislocation on radiative recombination of exciton and further explore the relationship between dislocation density and IQE of GaN-based semiconductors. Thus it can be predicted that to what extent the luminous efficiency of GaN-based semiconductors can still maintain when the dislocation density increases under different epitaxy platforms such as MOCVD and MBE, so as to provide a reasonable rule of thumb for optimizing the epitaxial growth of GaN-based devices.

In this paper, by analyzing the influence of dislocation on non-radiative recombination as well as the vector average effect of stress fields and charge fields of dislocations on radiative recombination of exciton, the relationship between IQE and dislocation density is obtained. Then combined with related experimental results, the trend of IQEs changing with dislocation density for bulk GaN and AlGaN multiple quantum wells (MQWs) with the same light emission wavelength are well fitted using this relationship and its simplified form, respectively. These results show that this model can be a good guiding role for the growth of GaN-based semiconductor devices.

II. THEORETICAL MODEL

In general, dislocations are thought to introduce deep energy levels in the forbidden band of semiconductors, and they can act as the carrier non-radiative recombination centres,[22,23] therefore the non-radiative recombination lifetime (τ_{nr}) of carrier can be related to the dislocation density (N) when ignoring other non-radiative recombination mechanisms such as surface states, interface states and Auger recombination under large injection. The schematic diagram of dislocation in GaN is presented in Fig. 1. It is assumed that the screw and edge dislocations in the GaN material are all uniformly distributed, the distance between adjacent dislocations is L, and the thermal motion velocity of carriers is v_{th}, then there is $\tau_{nr} \propto L/v_{th}$. Besides, according to the definition of dislocation density, $L^2 \times N = 1$. Combined with these two equations, it can be obtained that:

$$1/\tau_{nr} \propto v_{th} \times \sqrt{N} \tag{1}$$

The mixed-type dislocation can be divided into screw- and edge-types. Therefore 'edge dislocation' is used to represent the sum of pure edge-type and edge component of mixed-type dislocations, and 'screw dislocation' refers to the sum of pure screw-type and screw component of mixed-type dislocations.[24] Considering both the screw-type dislocation density (N_s) and the edge-type dislocation density (N_e), as well as the difference between their capture cross sections of non-radiative recombination centers, the total non-radiative recombination lifetime τ_{nr} can be expressed as:

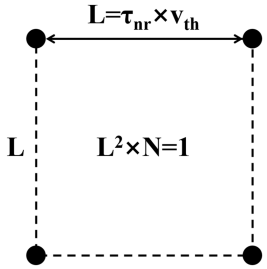

FIG. 1. Schematic diagram of dislocation in top view of c-plane GaN. Each black dot in the figure represents a dislocation extending to the surface.

$$1/\tau_{nr} = 1/\tau_{nr-screw} + 1/\tau_{nr-edge} = c_1\sqrt{N_s} + c_2\sqrt{N_e} \tag{2}$$

Where c_1 and c_2 are constants.

Because the exciton binding energy of GaN-based semiconductors is relatively high (20 ~ 28 meV),[25–28] exciton radiative recombination accounts for a significant proportion at room temperature. Exciton radiative recombination lifetime (τ_r) in ideal crystals can be expressed as the following form:[29]

$$1/\tau_r = \frac{8\pi\omega_{ex}}{\hbar c}|\phi(0)|^2\mu_{CV}{}^2 = 24\pi(\frac{\lambda_{ex}}{a_B})^2\gamma_S \tag{3}$$

Where $\gamma_S = \frac{4\mu_{CV}{}^2}{3\hbar\lambda_{ex}^3}$, ω_{ex} and λ_{ex} are respectively the exciton frequency and wavelength, c is the speed of light, $\phi(0)$ is the wave function of the exciton-internal-motion, μ_{CV}^2 is the transition probability, a_B is the exciton radius. It can be seen that exciton radiative recombination lifetime in ideal crystals is almost a constant under the same temperature and the same epitaxy structure.

In addition to serving as a non-radiative recombination centre, the dislocations also have significant influence on the radiative recombination of the excitons through the stress field ($\overrightarrow{E^{str}}$) and charge field ($\overrightarrow{E^{cha}}$) they caused. Due to the presence of these two fields of dislocations, the wave functions of electron and hole will separate in space, thus the radiative recombination lifetime of exciton will change.

Assuming that the polarization intensity vector caused by the stress fields of dislocations is $\vec{P}$, and the corresponding polarization electric field is $\overrightarrow{E^{str}}$, the relationship between them is $\vec{P} = \epsilon_0\overleftrightarrow{\chi_e}\cdot\overrightarrow{E^{str}} = \epsilon_0\left(\overleftrightarrow{\varepsilon}_r - 1\right)\cdot\overrightarrow{E^{str}}$, where ϵ_0 is the vacuum dielectric constant, $\overleftrightarrow{\chi_e}$ is polarizability tensor, $\overleftrightarrow{\epsilon_r}$ is relative permittivity tensor. In the hexagonal wurtzite structure, the polarizability tensor can be expressed as follows:

$$\overleftrightarrow{\chi_e} = \begin{bmatrix} \chi_{11} & 0 & 0 \\ 0 & \chi_{11} & 0 \\ 0 & 0 & \chi_{13} \end{bmatrix} \tag{4}$$

Thus, the three components of the polarized electric field intensity can be expressed as follows:

$$\begin{cases} E_x^{str} = \frac{1}{\varepsilon_0\chi_{11}}P_x \\ E_y^{str} = \frac{1}{\varepsilon_0\chi_{11}}P_y \\ E_z^{str} = \frac{1}{\varepsilon_0\chi_{13}}P_z \end{cases} \tag{5}$$

Besides, the polarization intensity vector $\vec{P}$ caused by the stress fields of dislocations can also be expressed as:[30]

$$\vec{P} = \overleftrightarrow{e}\cdot\vec{\varepsilon} = \begin{bmatrix} 0 & 0 & 0 & 0 & e_{15} & 0 \\ 0 & 0 & 0 & e_{24} & 0 & 0 \\ e_{31} & e_{31} & e_{33} & 0 & 0 & 0 \end{bmatrix} \begin{bmatrix} \varepsilon_{xx} \\ \varepsilon_{yy} \\ \varepsilon_{zz} \\ \varepsilon_{yx} \\ \varepsilon_{zx} \\ \varepsilon_{zy} \end{bmatrix} \tag{6}$$

Where $\vec{e}$ is the piezoelectric polarization tensor, and $\vec{\varepsilon}$ is the strain tensor. According to the request of symmetry, there is $e_{15} = e_{24}$ in the hexagonal crystal. From the above equation it can be obtained that:

$$\begin{cases} P_x = e_{15}\varepsilon_{zx} \\ P_y = e_{24}\varepsilon_{yx} \\ P_z = e_{31}\left(\varepsilon_{xx} + \varepsilon_{yy}\right) + e_{33}\varepsilon_{zz} = 2\left(e_{31} - e_{33}\frac{C_{13}}{C_{33}}\right)\varepsilon_{xx} \end{cases} \tag{7}$$

Where C_{13} and C_{33} are the elastic constants of the materials.

The material strain due to the dislocations can be expressed as:

$$\begin{cases} \varepsilon_{xx} = E^{-1}\sigma_{xx} \\ \varepsilon_{xx} = G^{-1}\tau_{yx} \\ \varepsilon_{zx} = G^{-1}\tau_{zx} \end{cases} \tag{8}$$

Where E and G are the elastic and shear modulus of the materials, respectively. σ_{xx} is the normal stress component, τ_{yx} and τ_{zx} are the shear stress components.

According to the theory of stress fields of dislocations, spatial expressions of σ_{xx}, τ_{yx} and τ_{zx} caused by screw and edge dislocations can be expressed as Eqs. (9) and (10), respectively.[31]

$$\begin{cases} \sigma_{xx} = 0 \\ \tau_{yx} = 0 \\ \tau_{zx} = -\dfrac{Gb}{2\pi}\dfrac{y}{x^2+y^2} \end{cases} \tag{9}$$

$$\begin{cases} \sigma_{xx} = -\dfrac{Gb}{2\pi(1-\upsilon)}\dfrac{y\left(3x^2+y^2\right)}{\left(x^2+y^2\right)^2} \\ \tau_{yx} = \dfrac{Gb}{2\pi(1-\upsilon)}\dfrac{x\left(x^2-y^2\right)}{\left(x^2+y^2\right)^2} \\ \tau_{zx} = 0 \end{cases} \tag{10}$$

Where b is the Burgers vector of dislocations, and υ is the Poisson's ratio of the materials. The schematic diagrams of screw and edge dislocation are shown in Fig. 2.[32]

Combining Eqs. (6), (7), (8), (9) and (10), the expressions for the stress fields of dislocations can be expressed as follows:

$$\begin{cases} E_x^{str} = \dfrac{1}{\epsilon_0\chi_{11}} e_{15} G^{-1} \dfrac{-Gb}{2\pi}\dfrac{y}{x^2+y^2} = -\dfrac{be_{15}}{2\pi\epsilon_0\chi_{11}} S_x \\ E_y^{str} = \dfrac{1}{\epsilon_0\chi_{11}} e_{24} G^{-1} \dfrac{Gb}{2\pi(1-\upsilon)}\dfrac{x\left(x^2-y^2\right)}{\left(x^2+y^2\right)^2} = \dfrac{e_{24}b}{2\pi\epsilon_0\chi_{11}(1-\upsilon)} S_y \\ E_z^{str} = \dfrac{1}{\epsilon_0\chi_{13}} 2\left(e_{31} - e_{33}\dfrac{C_{13}}{C_{33}}\right) E^{-1} \dfrac{-Gb}{2\pi(1-\upsilon)}\dfrac{y\left(3x^2+y^2\right)}{\left(x^2+y^2\right)^2} = \dfrac{-Gb}{\epsilon_0\chi_{13}\pi(1-\upsilon)E}\left(e_{31} - e_{33}\dfrac{C_{13}}{C_{33}}\right) S_z \end{cases} \tag{11}$$

Where S_x, S_y and S_z are the structural factors in stress field model. Here we put forward the vector average method of stress fields by taking the adjacent dislocations of a carrier or exciton into account.

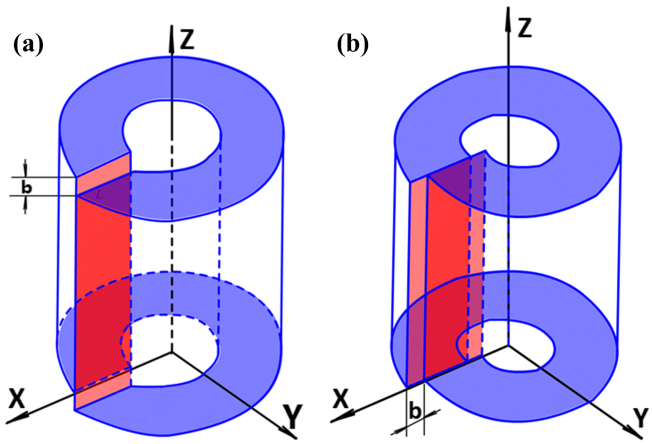

FIG. 2. The schematic diagrams of (a) screw and (b) edge dislocation. b is the Burgers vector of dislocations.

The electric field intensity of stress fields is averaged through vector summation of adjacent four dislocations (as shown in Fig. 1) of a carrier or exciton at an arbitrary position. Our simulation results reveal that the average of $\boldsymbol{S_x}$ is inversely proportional to the mean distance $\boldsymbol{L_s}$ between adjacent screw dislocations, and the average of either $\boldsymbol{S_y}$ or $\boldsymbol{S_z}$ is inversely proportional to the mean distance $\boldsymbol{L_e}$ between adjacent edge dislocations. Therefore, the components of average stress fields can be obtained according to Eq. (11):

$$\begin{cases} \overline{\boldsymbol{E_x^{str}}} = \boldsymbol{c_3}\sqrt{\boldsymbol{N_s}} \\ \overline{\boldsymbol{E_y^{str}}} = \boldsymbol{c_4}\sqrt{\boldsymbol{N_e}} \\ \overline{\boldsymbol{E_z^{str}}} = \boldsymbol{c_5}\sqrt{\boldsymbol{N_e}} \end{cases} \tag{12}$$

Where $\boldsymbol{c_3}$, $\boldsymbol{c_4}$ and $\boldsymbol{c_5}$ are constants. It can be seen that the components of stress fields of dislocations in the material are proportional to the square roots of the screw or edge dislocation densities.

In order to get the relationship between charge fields and edge dislocation densities, line charge at edge dislocation core due to dangling bonds can be considered as uniform. So the three components of the charge field intensity can be expressed as follows through simple derivation:

$$\begin{cases} \boldsymbol{E_x^{cha}} = \dfrac{\lambda}{2\pi\epsilon_0}\dfrac{x}{\boldsymbol{x^2+y^2}} = \dfrac{\lambda}{2\pi\epsilon_0}S_x' \\ \boldsymbol{E_y^{cha}} = \dfrac{\lambda}{2\pi\epsilon_0}\dfrac{y}{\boldsymbol{x^2+y^2}} = \dfrac{\lambda}{2\pi\epsilon_0}S_y' \\ \boldsymbol{E_z^{cha}} = 0 \end{cases} \tag{13}$$

Where $\boldsymbol{\lambda}$ is the linear charge density at edge dislocation core, which can be regarded as a constant when each dangling bond has already trapped electron. S_x' and S_y' are the structural factors in charge field model. Similar to the stress fields, the electric field intensity of charge fields is also averaged according to the same method. Our simulation results also reveal that the average S_x' and S_y' are all inversely proportional to the mean distance $\boldsymbol{L_e}$ between adjacent edge dislocations. So the components of average charge fields can be obtained according to Eq. (13):

$$\begin{cases} \overline{\boldsymbol{E_x^{cha}}} = \boldsymbol{c_6}\sqrt{\boldsymbol{N_e}} \\ \overline{\boldsymbol{E_y^{cha}}} = \boldsymbol{c_7}\sqrt{\boldsymbol{N_e}} \\ \overline{\boldsymbol{E_z^{cha}}} = 0 \end{cases} \tag{14}$$

Where $\boldsymbol{c_6}$ and $\boldsymbol{c_7}$ are constants. It can be seen that the components of charge fields of dislocations in the material are proportional to the square roots of the edge dislocation densities.

Because the effects of electric field on electron and hole wave functions cannot be expressed by a simple equation, we simulated the situations of 100-nm bulk GaN and 2-nm $In_{0.1}Ga_{0.9}N$/GaN QW as examples by applying electric fields along different directions. Using the **k·p** method, the wave functions of electron and hole under different electric fields can be obtained. According to the simulation results in the two structures illustrated using different symbols in Fig. 3(a) and Fig. 3 (b), the

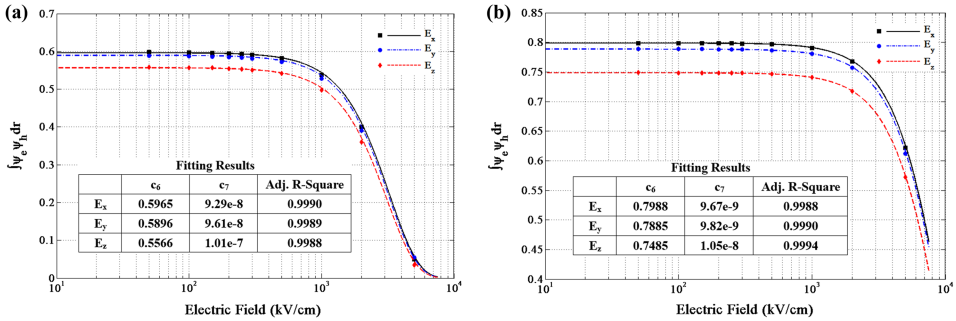

FIG. 3. The calculation and fitting results of the relationships between overlap integrals of the electron and hole wave functions and electric field in (a) 100-nm bulk GaN and (b) 2-nm $In_{0.1}Ga_{0.9}N$/GaN QW.

overlap integrals of the electron and hole wave functions at different applied electric field intensities can be fitted using Eq. (13) in both GaN-based bulk layer and QW,

$$\int \psi_e \psi_h dr = c_8 e^{-c_9 (E_i^{tot})^2} \tag{15}$$

Where ψ_e and ψ_h represent the wave functions of electron and hole, respectively, $E_i^{tot} (i = x, y, z)$ represents the total electric field strength (E_i^{tot}) = $\overline{E_i^{str}} + \overline{E_i^{cha}}$, $i = x, y, z$) in a certain direction. And c_8 and c_9 are constants. The fitting results are plotted using solid lines in Fig. 3.

The relationship between the dislocation density and the overlap integral of the wave functions can be further obtained from Eqs. (12), (14) and (15) as follows:

$$\int \psi_e \psi_h dr = c_8 e^{-c_9 \left((E_x^{tot})^2 + (E_y^{tot})^2 + (E_z^{tot})^2 \right)} = c_8 e^{-\left(c_{10} N_s + c_{11} N_e + c_{12} \sqrt{N_s N_e} \right)} \tag{16}$$

Where c_{10}, c_{11} and c_{12} are constants.

Because the radiative recombination lifetime τ_r is inversely proportional to the radiation recombination rate which is proportional to the overlap of the electron and hole wave functions,[33] the effect of dislocations on the radiative recombination lifetime can be obtained as follows:

$$\tau_r' = \tau_r \, c_8 e^{-\left(c_{10} N_s + c_{11} N_e + c_{12} \sqrt{N_s N_e} \right)} \tag{17}$$

Where τ_r' is the actual radiation recombination rate after correction, and τ_r is the ideal radiation recombination rate including the same spontaneous polarization effect regardless of the stress fields and charge fields of dislocations. $c_8 e^{-\left(c_{10} N_s + c_{11} N_e + c_{12} \sqrt{N_s N_e} \right)}$ can be regarded as the influence factor of dislocations on the radiation recombination rate.

According to the definition of IQE expressed as:[34]

$$\eta_{\mathrm{IQE}} (N_s, N_e) = \frac{1}{1 + \frac{\tau_{r'}}{\tau_{nr}}} \tag{18}$$

and substituting Eqs. (2) and (17) into Eq. (18), the following relationship can be obtained:

$$\eta_{IQE} (N_s, N_e) = \frac{1}{1 + (c_{13} \sqrt{N_s} + c_{14} \sqrt{N_e}) e^{c_{10} N_s + c_{11} N_e + c_{12} \sqrt{N_s N_e}}} \tag{19}$$

Where c_{13} and c_{14} are two constants to be fitted. Eq. (19) reveals the relationship between IQE and the densities of screw and edge dislocations. From this equation it can be thought that with the increase of screw and edge dislocation densities, the internal quantum efficiency of the materials has a process of rapid decline after the first slow decline.

III. EXPERIMENTAL RESULTS AND DISCUSSION

In this part, the model is used to fit some experimental results. Firstly, a series of bulk GaN samples with different dislocation densities were prepared on c-plane sapphire substrates by MOCVD growth. All samples were grown using a two-step process, namely a 3.5 μm-thick GaN bulk layer grown on a 30 nm-thick low-temperature GaN buffer layer. By changing the annealing time of the GaN buffer layer, samples with different dislocation densities were obtained. All samples were subjected to temperature-dependent photoluminescence (TDPL) measurements to obtain their IQEs.[35,36] Then X-ray diffraction measurements were performed to get the screw and edge dislocation densities of different samples under the assumption that the dislocations are uniformly distributed in the material.[37–39] Then the "IQE-dislocation density" relationship is fitted using Eq. (19). The fitting results show the Adj. R-Square has a value of 0.9974, which shows that the fitting curve is consistent well with the experimental data. The fitting results are shown in Fig. 4. The color of the experimental data points represents the amount of error between the experimental and fitting values. It can be seen that most of the experimental data are in good agreement with the theoretical model. Moreover, IQE decreases with the increasing of screw and edge dislocation densities. When the dislocation density is less than 1×10^8 cm^{-2}, IQE decreases slowly with the dislocation density; while IQE decreases rapidly when the dislocation density is between $1 \times 10^8 \sim 5 \times 10^9$ cm^{-2}. When the dislocation density of bulk GaN reaches 8×10^8 cm^{-2}, IQE can maintain 50%; when the dislocation density is as high

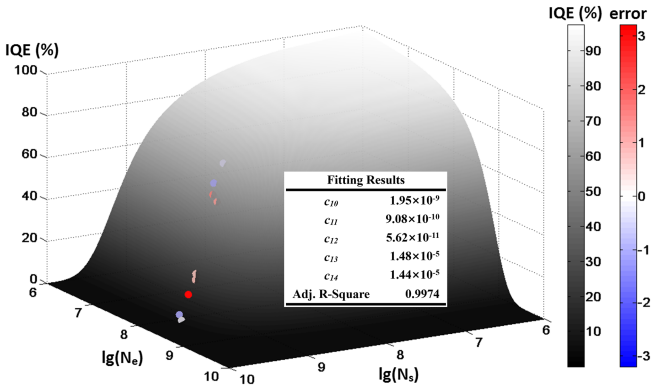

FIG. 4. The relationship between IQE of bulk GaN and screw dislocation (N_s) as well as edge dislocation density (N_e). The thickness of bulk GaN are all 3.5 μm. The left color bar corresponds to the IQE value of the fitted surface. The right color bar corresponds to the amount of error between the experimental and fitting values.

as 2.4×10^9 cm^{-2}, IQE can still reach 10%. This result illustrates the advantage of wide-band-gap GaN-based semiconductors in fabrication of optoelectronic devices. It is because that the exciton is stable at room temperature,[40] high efficiency of excitonic radiation recombination can be attributed to high exciton binding energy of GaN-based semiconductors even under high dislocation density. Other III-V semiconductors with narrow band gap (such as GaAs and InP) do not have this feature.

It was also reported in previous literatures that AlGaN MQW LEDs have different IQEs at different threading dislocation densities under the same light emission wavelength (~280nm),[41] thus the misfit stresses of different samples play the same role and can also fall under the ideal radiation recombination rate τ_r. The threading dislocation density is usually measured by chemical etching method since etch pits will appear at the positions of threading dislocations after selective wet etching,[42] and the density can be obtained directly by SEM observation. But in this way it is impossible to distinguish the screw dislocation and the edge dislocation. It can be observed that in Fig. 4 all the experimental data points are approximately distributed in the same cross section through the IQE coordinates, which indicates that the ratio of screw and edge dislocations is approximately fixed. In such a circumstance, it can be assumed that there is a relatively fixed ratio of screw and edge dislocations, and Eq. (19) can be simplified to the following form:

$$\eta_{IQE}(N) = \frac{1}{1 + c_{15}\sqrt{N}\, e^{c_{16}N}} \tag{20}$$

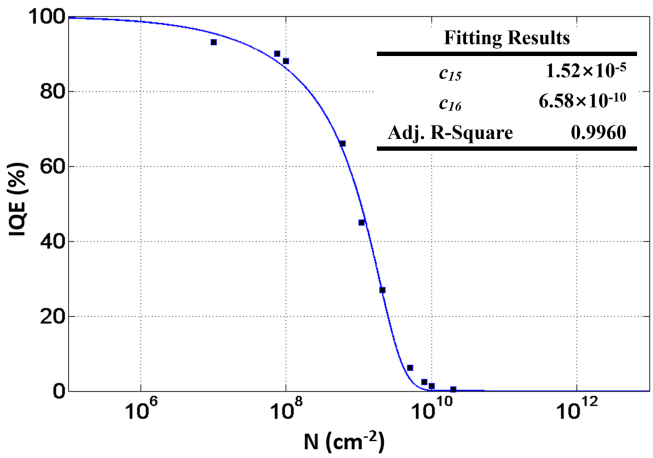

FIG. 5. The relationship between IQE of AlGaN MQWs LEDs and threading dislocation density (N). The black squares represent the experimental data. The blue solid line is the fitting curve.

Where N is the threading dislocation density obtained by chemical etching method, c_{15} and c_{16} are two constants to be fitted.

Then the data of the AlGaN MQW LEDs in Ref. 37 are fitted using Eq. (20). The fitting results are shown in Fig. 5, with an Adj. R-Square value of 0.9960. As can be seen from Fig. 5, the fitting curve can well reflect the variation of IQE with the threading dislocation density. Furthermore, when the dislocation density of the AlGaN MQW reaches 1.1×10^9 cm^{-2}, IQE can reach 50%. And when the dislocation density of the AlGaN MQWs is as high as 3.7×10^9 cm^{-2}, IQE can still reach 10%. Thus it can be seen that AlGaN MQWs are more tolerant to dislocations than bulk GaN, which is due to the quantum confinement effect of QW as well as larger exciton binding energy in QW compared to that in bulk materials.[43] So the probability of exciton radiation recombination before the carriers being captured by threading dislocations will be higher in QW than that in bulk materials.

IV. CONCLUSION

By analyzing the influence of dislocation on non-radiative recombination as well as the vector average effect of stress fields and charge fields of dislocations on radiative recombination of exciton, the relationship between IQE and dislocation density in GaN-based materials is obtained. Combined with related experimental results, this relationship is fitted well to the trend of IQEs of bulk GaN changing with screw and edge dislocation density, meanwhile its simplified form is fitted well to the IQEs of AlGaN MQW LEDs with varied threading dislocation density under the same light emission wavelength. It is believed that this model can be used to predict to what extent the luminous efficiency of GaN-based semiconductors can still maintain when the dislocation density increases, so as to provide a reasonable rule of thumb for optimizing the epitaxial growth of GaN-based devices. In addition, the model can also be used in other semiconductor materials with large exciton binding energy (such as ZnO and InGaN MQWs) to provide guidance for the development of semiconductor optoelectronic devices based on these materials.

ACKNOWLEDGMENTS

This work was supported by National Basic Research Program of China (Grant No. 2013CB632804), the National Key Research and Development Plan (Grant No. 2016YFB0400102), the National Natural Science Foundation of China (Grant Nos. 61574082, 61210014, 61321004, 61307024, 51561145005 and 51561165012), the High Technology Research and Development Program of China (Grant No. 2015AA017101), Tsinghua University Initiative Scientific Research Program (Grant Nos. 2013023Z09N, 2015THZ02-3), the Open Fund of the State Key Laboratory on Integrated Optoelectronics (Grant No. IOSKL2015KF10), the CAEP Microsystem and THz Science and Technology Foundation (Grant No. CAEPMT201505) and the Science Challenge Project (Grant No. JCKY2016212A503), Collaborative Innovation Center of Solid-State Lighting and Energy-Saving Electronics.

[1] M. R. Krames, O. B. Shchekin, R. Mueller-Mach, G. O. Mueller, L. Zhou, G. Harbers, and M. G. Craford, J. Disp. Technol. **3**, 160 (2007).
[2] S. Nakamura, M. Senoh, S. Nagahama, N. Iwasa, T. Yamada, T. Matsushita, H. Kiyoku, and Y. Sugimoto, Jpn. J. Appl. Phys. **35**, L74 (1996).
[3] R. Dahal, B. Pantha, J. Li, J. Y. Lin, and H. X. Jiang, Appl. Phys. Lett. **94**, 063505 (2009).
[4] J. M. Van Hove, R. Hickman, J. J. Klaassen, P. P. Chow, and P. P. Ruden, Appl. Phys. Lett. **70**, 2282 (1997).
[5] S. T. Sheppard, K. Doverspike, W. L. Pribble, S. T. Allen, J. W. Palmour, L. T. Kehias, and T. J. Jenkins, IEEE Electron Device Lett. **20**, 161 (1999).
[6] S. Lee, H. Jeong, S. Bae, H. Choi, J. Lee, and Y. Lee, IEEE Trans. Electron Devices **48**, 524 (2001).
[7] L. S. McCarthy, I. P. Smorchkova, H. Xing, P. Kozodoy, P. Fini, J. Limb, D. L. Pulfrey, J. S. Speck, M. J. Rodwell, and S. P. DenBaars, IEEE Trans. Electron Devices **48**, 543 (2001).
[8] B. Lu, E. Matioli, and T. Palacios, IEEE Electron Device Lett. **33**, 360 (2012).
[9] S. Nakamura, Y. Harada, and M. Seno, Appl. Phys. Lett. **58**, 2021 (1991).
[10] P. Schlotter, R. Schmidt, and J. Schneider, Appl. Phys. A **64**, 417 (1997).
[11] A. Dadgar, C. Hums, A. Diez, J. Bläsing, and A. Krost, J. Cryst. Growth **297**, 279 (2006).
[12] L. Wang, J. Wang, H. Li, G. Xi, Y. Jiang, W. Zhao, Y. Han, and Y. Luo, Appl. Phys. Express **1**, 021101 (2008).
[13] T. Hino, S. Tomiya, T. Miyajima, K. Yanashima, S. Hashimoto, and M. Ikeda, Appl. Phys. Lett. **76**, 3421 (2000).
[14] S. Y. Karpov and Y. N. Makarov, Appl. Phys. Lett. **81**, 4721 (2002).
[15] H. Zhao, G. Liu, R. A. Arif, and N. Tansu, Solid-State Electron. **54**, 1119 (2010).

[16] X. Meng, L. Wang, Z. Hao, Y. Luo, C. Sun, Y. Han, B. Xiong, J. Wang, and H. Li, Appl. Phys. Lett. **108**, 013501 (2016).
[17] J. Abell and T. D. Moustakas, Appl. Phys. Lett. **92**, 081916 (2008).
[18] Q. Dai, M. F. Schubert, M. Kim, J. K. Kim, E. F. Schubert, D. D. Koleske, M. H. Crawford, S. R. Lee, A. J. Fischer, and G. Thaler, Appl. Phys. Lett. **94**, 111109 (2009).
[19] I. Lu, Y. Wu, and J. Singh, J. Appl. Phys. **108**, 124508 (2010).
[20] P. Maree, J. C. Barbour, J. F. Van der Veen, K. L. Kavanagh, C. Bulle Lieuwma, and M. Viegers, J. Appl. Phys. **62**, 4413 (1987).
[21] D. Li, X. Sun, H. Song, Z. Li, Y. Chen, G. Miao, and H. Jiang, Appl. Phys. Lett. **98**, 011108 (2011).
[22] T. Sugahara, H. Sato, M. Hao, Y. Naoi, S. Kurai, S. Tottori, K. Yamashita, K. Nishino, L. T. Romano, and S. Sakai, Jpn. J. Appl. Phys. **37**, L398 (1998).
[23] D. Cherns, S. J. Henley, and F. A. Ponce, Appl. Phys. Lett. **78**, 2691 (2001).
[24] J. C. Zhang, D. G. Zhao, J. F. Wang, Y. T. Wang, J. Chen, J. P. Liu, and H. Yang, J. Cryst. Growth **268**, 24 (2004).
[25] J. F. Muth, J. H. Lee, I. K. Shmagin, R. M. Kolbas, H. C. Casey, Jr., B. P. Keller, U. K. Mishra, and S. P. DenBaars, Appl. Phys. Lett. **71**, 2572 (1997).
[26] W. Shan, B. D. Little, A. J. Fischer, J. J. Song, B. Goldenberg, W. G. Perry, M. D. Bremser, and R. F. Davis, Phys. Rev. B **54**, 16369 (1996).
[27] A. K. Viswanath, J. I. Lee, D. Kim, C. R. Lee, and J. Y. Leem, Phys. Rev. B **58**, 16333 (1998).
[28] B. Monemar, Phys. Rev. B **10**, 676 (1974).
[29] E. Hanamura, Phys. Rev. B **38**, 1228 (1988).
[30] H. Morkoç, *Nitride Semiconductor Devices: Fundamentals and Applications* (Wiley, Weinheim, 2013), p. 33.
[31] C. Kittel, *Introduction to Solid State Physics* (Wiley, Hoboken, 2005), p. 605.
[32] W. Zhao, L. Wang, J. Wang, Z. Hao, and Y. Luo, J. Appl. Phys. **110**, 014311 (2011).
[33] J. Bellessa, V. Voliotis, R. Grousson, X. L. Wang, M. Ogura, and H. Matsuhata, Phys. Rev. B **58**, 9933 (1998).
[34] H. Zhao, G. Liu, J. Zhang, R. A. Arif, and N. Tansu, J. Disp. Technol. **9**, 212 (2013).
[35] D. Fuhrmann, T. Retzlaff, U. Rossow, H. Bremers, A. Hangleiter, G. Ade, and P. Hinze, Appl. Phys. Lett. **88**, 1108 (2006).
[36] S. Watanabe, N. Yamada, M. Nagashima, Y. Ueki, C. Sasaki, Y. Yamada, T. Taguchi, K. Tadatomo, H. Okagawa, and H. Kudo, Appl. Phys. Lett. **83**, 4906 (2003).
[37] V. Srikant, J. S. Speck, and D. R. Clarke, J. Appl. Phys. **82**, 4286 (1997).
[38] S. R. Lee, A. M. West, A. A. Allerman, K. E. Waldrip, D. M. Follstaedt, P. P. Provencio, D. D. Koleske, and C. R. Abernathy, Appl. Phys. Lett. **86**, 241904 (2005).
[39] T. Metzger, R. Höpler, E. Born, O. Ambacher, M. Stutzmann, R. Stömmer, M. Schuster, H. Göbel, S. Christiansen, and M. Albrecht, Philos. Mag. A **77**, 1013 (1998).
[40] A. K. Viswanath, J. I. Lee, D. Kim, C. R. Lee, and J. Y. Leem, Phys. Rev. B **58**, 16333 (1998).
[41] M. Kneissl, T. Kolbe, C. Chua, V. Kueller, N. Lobo, J. Stellmach, A. Knauer, H. Rodriguez, S. Einfeldt, and Z. Yang, Semicond. Sci. Technol. **26**, 014036 (2010).
[42] T. Hino, S. Tomiya, T. Miyajima, K. Yanashima, S. Hashimoto, and M. Ikeda, Appl. Phys. Lett. **76**, 3421 (2000).
[43] S. Nakamura and S. F. Chichibu, *Introduction to Nitride Semiconductor Blue Lasers and Light Emitting Diodes* (CRC Press, New York, 2000), p. 191.